J|A|C|S ARTICLES

Published on Web 05/06/2009

Staphylococcus aureus Peptidoglycan Tertiary Structure from Carbon-13 Spin Diffusion

Shasad Sharif, Manmilan Singh, Sung Joon Kim, and Jacob Schaefer*

Department of Chemistry, Washington University, St. Louis, Missouri 63130

Received November 14, 2008; E-mail: jschaefer@wustl.edu

Abstract: The cell-wall peptidoglycan of *Staphylococcus aureus* is a heterogeneous, highly cross-linked polymer of unknown tertiary structure. We have partially characterized this structure by measuring spin diffusion from ^{13}C labels in pentaglycyl cross-linking segments to natural-abundance ^{13}C in the surrounding intact cell walls. The measurements were performed using a version of centerband-only detection of exchange (CODEX). The cell walls were isolated from *S. aureus* grown in media containing [1-^{13}C]glycine. The CODEX spin diffusion rates established that the pentaglycyl bridge of one peptidoglycan repeat unit of *S. aureus* is within 5 Å of the glycan chain of another repeat unit. This surprising proximity is interpreted in terms of a model for the peptidoglycan lattice in which all peptide stems in a plane perpendicular to the glycan mainchain are parallel to one another.

Introduction

The peptidoglycan in *Staphylococcus aureus* is typically 20-30 nm thick[1] and serves as a protective barrier, as well as a scaffold for the attachment of surface proteins and extracellular matrices, which are required for cell morphogenesis, cell division, and pathogenesis. The peptidoglycan is assembled from a repeat unit consisting of disaccharide, stem, and bridge. The disaccharide, *N*-acetylglucosamine and *N*-acetylmuramic acid, is conserved in all bacteria, but the stem and bridge structures vary from one organism to another.[2] In *S. aureus*, the stem is the pentapeptide, L-alanine-D-*iso*-glutamine-L-lysine-D-alanine-D-alanine, and the bridge is a pentaglycyl segment. The chemical structure of the *S. aureus* peptidoglycan is shown in Scheme 1.

The final assembly of peptidoglycan involves the action of two essential enzymes, transglycosylase[3] and transpeptidase,[4] at the exoface of the cytoplasmic membrane. Transglycosylase catalyzes the formation of a $\beta(1-4)$ glycosidic bond between the disaccharides of glycan units thereby forming a polymerized glycan mainchain. The newly formed glycan chain, often referred to as the nascent peptidoglycan, is incorporated into the surrounding cell wall by transpeptidase. Transpeptidase mediates the formation of a cross-link, a peptide bond between the *N*-terminus of the terminal glycine of the pentaglycyl segment attached to one stem, and the D-alanine of a neighboring pentapeptide stem (D-Ala_4), as illustrated in Scheme 1. The result of transglycosylase and transpeptidase activity is the formation of a three-dimensional peptidoglycan lattice which encapsulates the entire organism.[5,6]

The peptidoglycan in *S. aureus* is large, insoluble, and heterogeneous, making it incompatible with conventional structural methods, such as X-ray crystallography, neutron diffraction, and liquid-state NMR. Despite its known chemical structure, the peptidoglycan tertiary structure remains largely unknown. We have already reported on the incorporation of specific ^{13}C, ^{15}N, and ^{2}H labels into the stems and bridges of *S. aureus* peptidoglycan, and the measurement of distances between the labels,[7] and from these labels to the ^{19}F of glycopeptide drugs bound to the cell walls,[8] by rotational-echo double-resonance (REDOR)[9] NMR. However, none of these measurements specified the location of the labels relative to the glycan chains. In this report, we describe the use of ^{13}C spin diffusion from ^{13}C-labeled pentaglycyl bridging segments to nearby natural-abundance ^{13}C in the glycan mainchain to measure bridge-glycan distances and so help define the peptidoglycan lattice architecture in *S. aureus* strain BB255,[10] in its isogenic *femA*-deletion mutant, UK 17,[11] and in the vancomycin-intermediate resistant *S. aureus* mutant, Mu50.[12]

Experimental Section

Growth and Labeling of Peptidoglycan. Starter cultures of *S. aureus* BB255,[10a,b] *FemA* (UK 17),[11a−c] and Mu50[12] were grown by inoculating 5 mL of trypticase soy broth (TSB) in a test tube

(1) Giesbrecht, P.; Kersten, T.; Maidhof, H.; Wecke, J. *Microb. Mol. Biol. R.* **1998**, *62*, 1371–1414.
(2) Rogers, H. J., Perkins, H. R., Ward, J. B. *Microbial Cell Walls and Membranes*; Chapman and Hall: London, 1980.
(3) Labischinski, H. *Med. Microbiol. Immunol.* **1992**, *181*, 241–265.
(4) de Lencastre, H.; Jonge, B. L. M.; Matthews, P. R.; Tomasz, A. *J. Antimicrob. Chemoth.* **1994**, *33*, 7–14.
(5) Labischinski, H.; Barnickel, G.; Bradaczek, H.; Giesbrecht, P. *Eur. J. Biochem.* **1979**, *95*, 147–155.
(6) van Heijenoort, J. *Glycobiology* **2001**, *11*, 25R–36R.
(7) (a) Tong, G.; Pan, Y.; Dong, H.; Pryor, R.; Wilson, G. E.; Schaefer, J. *Biochemistry* **1997**, *36*, 9859–9866. (b) Mehta, A. K.; Cegelski, L.; O'Connor, R. D.; Schaefer, J. *J. Magn. Reson.* **2003**, *163*, 182–187.
(8) (a) Kim, S. J.; Cegelski, L.; Studelska, D. R.; O'Connor, R. D.; Mehta, A. K.; Schaefer, J. *Biochemistry* **2002**, *41*, 6967–6977. (b) Kim, S. J.; Cegelski, L.; Preobrazhenskaya, M.; Schaefer, J. *Biochemistry* **2006**, *45*, 5235–5250. (c) Cegelski, L.; Stueber, D.; Mehta, A. K.; Kulp, D. W.; Axelsen, P. H.; Schaefer, J. *J. Mol. Biol.* **2006**, *357*, 1253–1262. (d) Kim, S. J.; Cegelski, L.; Stueber, D.; Singh, M.; Dietrich, E.; Tanaka, K. S. E.; Parr, T. R., Jr.; Far, A. R.; Schaefer, J. *J. Mol. Biol.* **2008**, *377*, 281–293. (e) Kim, S. J.; Matsuoka, S.; Patti, G. J.; Schaefer, J. *Biochemistry* **2008**, *47*, 3822–3831. (f) Kim, S. J.; Schaefer, J. *Biochemistry* **2008**, *47*, 10155–10161.
(9) (a) Gullion, T.; Schaefer, J. *Adv. Magn. Reson.* **1989**, *13*, 57–83. (b) Gullion, T.; Schaefer, J. *J. Magn. Reson.* **1989**, *81*, 196–200.

Scheme 1. (a) Chemical Structure of the Peptidoglycan of *Staphylococcus aureus* and Two of Its Mutants.[a] (b) Expansion of the Cross-Link to Bridge-Link Structure

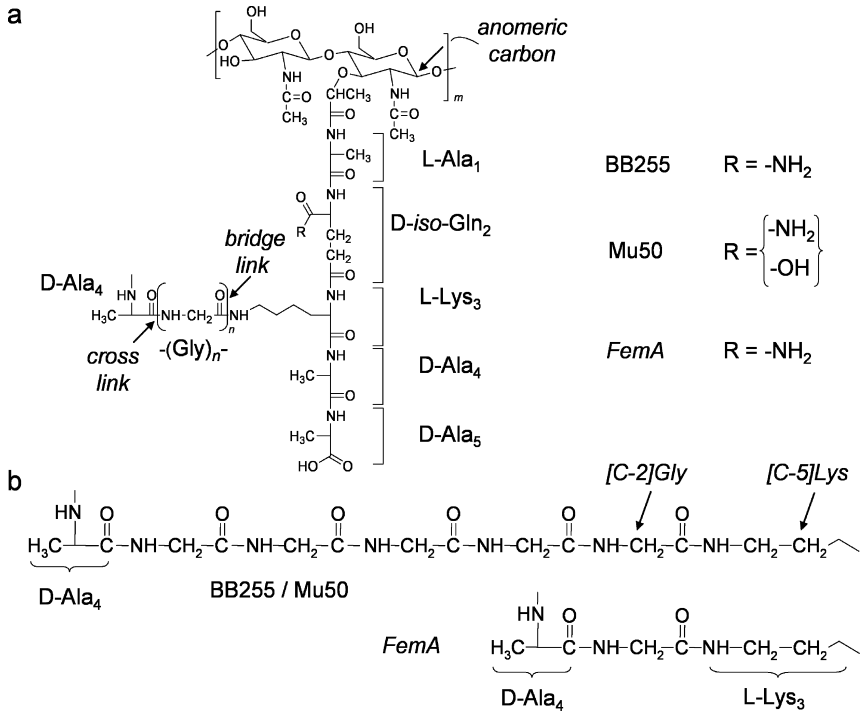

[a] The partial stem on the left contains a D-Ala-Gly cross-link (peptide bond), and the full stem on the right, a Gly-L-Lys (isopeptide bond) bridge-link. The bridging glycyl segment is attached to the L-Lys of the stem on the right, which ends in a D-Ala-D-Ala vancomycin binding site. The glycine content in the side chain differs from $n = 5$ (*S. aureus* strains BB255 and mutant Mu50) to $n = 1$ (*FemA*).

with a single colony obtained from a nutrient agar plate. The starter cultures were shaken at 200 rpm in an Environ-Shaker (Laboratory-Lines Instruments, Inc., Melrose Park, IL), maintained overnight at 37 °C, but not aerated. The overnight starter culture (1% final volume) was added to 2 L sterile *S. aureus* standard medium (SASM), in six 1 L flasks each containing 330 mL. SASM, as described earlier by Tong et al.,[7a] contained the following on a per-liter basis: 10 g of D(+)glucose; 1 g each of $K_2HPO_4 \cdot 3H_2O$, KH_2PO_4, and $(NH_4)_2SO_4$; 0.2 g of $MgSO_4 \cdot 7H_2O$; 10 mg each of $MnSO_4 \cdot H_2O$, $FeSO_4 \cdot H_2O$, and NaCl; 5 mg each of adenine, cytosine, guanine, uracil, and xanthine; 2 mg each of thiamine·HCl (vitamin B_1), niacin (vitamin B_3), and calcium pantothenate (vitamin B_5); 1 mg each of riboflavin (vitamin B_2), pyridoxine·HCl (vitamin B_6), inositol, $CuSO_4 \cdot 5H_2O$, and $ZnSO_4 \cdot 7H_2O$; 0.1 mg each of biotin (vitamin B_7) and folic acid (vitamin B_9); and 0.1 g of all 20 common amino acids. The pH of SASM was adjusted to 7.0 with 1 M KOH, followed by sterile filtration (0.22 μm membrane). The natural-abundance amino acids in SASM were replaced by either 99%-enriched [1-^{13}C]glycine or 5%-enriched [1-^{13}C]glycine to incorporate specific ^{13}C label into the glycyl carbonyl carbon in the peptidoglycan (PG) (Scheme 1). The isotopic labeled amino acids were purchased from Isotec.

The cells were harvested at log-phase, at an optical density O.D. of 0.6 (BB255 and *FemA*) and 1.0 (Mu50) at 660 nm, by centrifugation at 10 000*g* for 10 min at 4 °C in a Sorvall GS-3 rotor. Cell pellets were rinsed twice with 300 mL of ice-cold 40 mM triethanolamine hydrochloride (pH 7.0, adjusted with 1 M NaOH). The rinsed pellets were resuspended in a minimum amount of the same buffer followed by rapid freezing and lyophilization.

Cell-wall isolates were prepared from lyophilized whole cells as previously described.[7a] Lyophilized cells from the 2 L of log-phase growth were resuspended in 100 mL of sterile 0.025 M potassium phosphate buffer (pH 7.0), boiled for 30 min, and then chilled on an ice bath. To the cell suspension, DNase I (type II; from bovine pancreas, Sigma-Aldrich, 1 mg per 100 mg dry cell weight) was added and the mixture was transferred to a 250 mL Bead-Beater (Biospec Products, Bartlesville, OK) chamber, containing one-third (by volume) 0.5-mm diameter glass beads. Cell disruption employed ten 1-min cycles separated by 1-min cooling periods at 0 °C. Glass beads were separated from the broken cells with a coarse sintered glass funnel (20 μm) and were washed with 1 L of 10 mM EDTA. Centrifugation of the filtrate at 10 000*g* for 1 h at 4 °C provided crude cell walls. A suspension of the crude cell-wall pellet in a minimum amount of sterile 10 mM triethanolamine hydrochloride buffer (pH 7.0) was added dropwise with stirring to 100 mL of boiling 4% sodium dodecyl sulfate (SDS). After boiling for 30 min, the suspension was allowed to cool for 2 h with stirring, after which it was allowed to stand unstirred overnight at room temperature, and then sedimented by centrifugation at 38 000*g* for 1 h at room temperature in a Sorvall SS-34 rotor. Cell walls were rinsed with 100 mL of buffer at least four times, with centrifugation after each rinse, until no SDS could be detected. The pellet was resuspended in 60 mL of 0.01 M Tris buffer, pH 8.2, containing 1 mg per 100 mg dry cell weight DNase I, 3.2 mg per 100 mg dry cell weight of trypsin (type II-S; from bovine pancreas, Sigma-Aldrich), and α-chymotrypsin (type II; from bovine pancreas, Sigma-Aldrich). The suspension was incubated at 37 °C and shaken at 150 rpm in an Environ-Shaker for 16 h, sedimented at 38 000*g* for 1 h at 20 °C, and washed at least four times with buffer, with centrifugation after each rinse. Cells were then resuspended in a minimum amount of 10 mM triethanolamine buffer followed by rapid freezing and lyophilization. The resulting cell-wall isolates weighed ~150 mg.

(10) (a) Berger-Bächi, B. *J. Bacteriol.* **1983**, *154*, 479–487. (b) Berger-Bächi, B.; Kohler, M. L. *FEMS Microbiol. Lett.* **1983**, *20*, 305–309.
(11) (a) Maidhof, H.; Reinicke, B.; Blümel, P.; Berger-Bächi, B.; Labischinski, H. *J. Bacteriol.* **1991**, *173*, 3507–3513. (b) Kopp, U.; Roos, M.; Wecke, J.; Labischinski, H. *Microb. Drug Resist.* **1996**, *2*, 29–41. (c) Ehlert, K.; Schröder, W.; Labischinski, H. *J. Bacteriol.* **1997**, *179*, 7573–7576.
(12) Hiramatsu, K.; Hanaki, H.; Ino, T.; Yabuta, K.; Oguri, T.; Tenover, F. C. *J. Antimicrob. Chemother.* **1997**, *40*, 135–136.

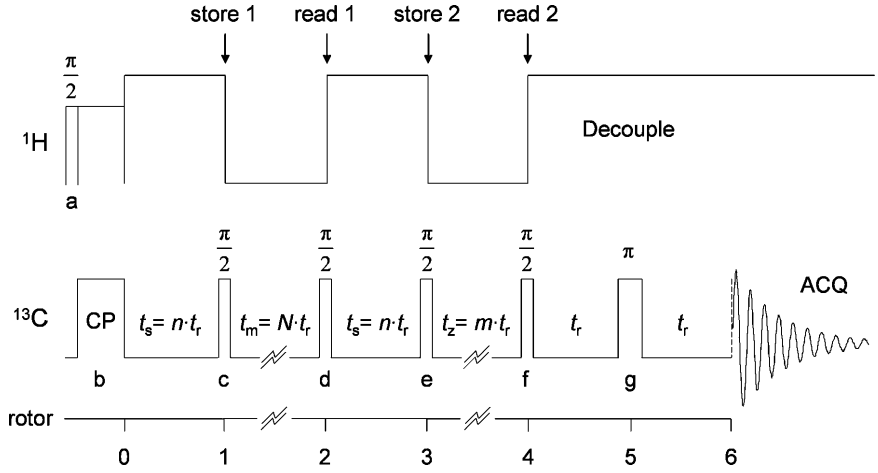

Figure 1. Pulse sequence for measurement of ^{13}C spin diffusion by CODEX. All times are multiples of the rotor period, t_r. When t_m occurs between the first pair of store-and-read 90° pulses and t_z between the second pair (as illustrated), the acquired signal is S. When the positions of t_m and t_z are interchanged, the acquired signal is S_0. The sum of t_m and t_z is a constant. Phases of the pulses are given in Table 1.

Table 1. Phases for the CODEX pulse sequence of Figure 1

pulse location	description	phase
a	^{1}H 90°	$(+x - x)^{64}$
b	^{1}H CP	$(+y)^{128}$
b	^{13}C CP	$(+x)^{128}$
c	first store ^{13}C 90°	$((-y)^8(-x)^8(+y)^8(+x)^8)^4$
d	first readout ^{13}C 90°	$((+y)^8(+x)^8)^2((-y)^8(-x)^8)^2$ $((-x)^8(+y)^8)^2((+x)^8(-y)^8)^2$
e	second store ^{13}C 90°	$(-y)^{64}(-x)^{64}$
f	second readout ^{13}C 90°	$((+y)^2(-x)^2(-y)^2(+x)\ ^2)^{16}$
g	^{13}C Hahn echo 180°	$(+x)^{128}$
ACQ	^{13}C signal acquisition	(02132031)(20310213) $((20310213)(02132031))^2$ (02132031)(20310213) (20310213)(02132031) $((02132031)(20310213))^2$ (20310213)(02132031)

Pulse Sequence for CODEX. The protocol for the measurement of ^{13}C spin diffusion uses a version of centerband-only detection of exchange (CODEX). The sequence for the delays and pulses is shown in Figure 1,[13] and the phases for the pulses in Table 1.[13c] When t_m occurs between the first pair of store-and-read 90° pulses and t_z between the second pair (as illustrated in Figure 1), the acquired signal is S. When the positions of t_m and t_z are interchanged, the acquired signal is S_0. CODEX is a constant-time experiment (the sum of t_m and t_z is the same for both S and S_0) which is $T_1(C)$ relaxation compensated;[13a] that is, changes in carbon signal intensities due to spin-lattice relaxation during the mixing time are not included in the CODEX difference ($\Delta S = S_0 - S$).

In the experiments reported here all times are multiples of t_r (the rotor period), $t_m = Nt_r$ and was hundreds of ms, $t_z = mt_r$ and was a few ms, and $t_s = nt_r$ with $n = 1$ and $t_r = 140$ μs (Figure 1). The timing of the d and f pulses was triggered externally by detection of the position of the rotor.[13] The parameters N, m, and n were integers with $N \gg m$. If n is not fixed but incremented, the resulting two-dimensional CODEX differences establish the chemical shifts of the spins engaged in exchange.[14] However, for spin exchange between specific ^{13}C labels and natural-abundance ^{13}C, the chemical shifts of coupled pairs are already known, and one-dimensional CODEX is preferred because of its time-saving advantage.

In standard CODEX, ^{13}C π pulses during the preparation time, t_s, create chemical-shift-tensor coherences that are stored prior to the mixing time and then recalled after the mixing time. If the shift-tensor orientation has remained unchanged during the mixing time, the ^{13}C π pulses during the second t_s period result in a full-size signal that is stored, recovered, and detected as a Hahn echo. The same Hahn echo is observed regardless of whether t_m proceeds or follows t_z ($S_0 = S$). However, if molecular or spin dynamics occur during t_m but not during the much shorter t_z, refocusing is incomplete and ΔS is nonzero.[13,15]

In the CODEX experiment of Figure 1, there are no pulses during t_s, the store and read $\pi/2$ pulses are rotor synchronized, and the effects of changes in shift-tensor orientations are removed by magic-angle spinning. However, changes in isotropic chemical shifts during t_m contribute to ΔS, and in solids such changes are almost always due to spin diffusion (flip-flop spin exchange within $^{13}C-^{13}C$ pairs), not molecular exchange. ^{13}C spin diffusion is sometimes enhanced by low-level proton irradiation during the mixing time,[16] but for relatively slow 7-kHz magic-angle spinning, this step is not necessary for diffusion over distances of the order of 5 Å in 1 s.[17]

Spectrometer. Experiments were performed at 12 T with a six-frequency transmission-line probe[18] having a 12-mm long, 6-mm inside-diameter analytical coil, and a Chemagnetics/Varian ceramic spinning module. Samples were spun using a thin-wall Chemagnetics/Varian (Fort Collins, CO/Palo Alto, CA) 5-mm outside diameter-zirconia rotor at 7143 Hz, with the speed under active control and maintained to within ±2 Hz. A Tecmag Libra pulse programmer (Houston, TX) controlled the spectrometer. A 2-kW American Microwave Technology power amplifier was used to produce radio frequency pulses for ^{13}C (125 MHz). The ^1H (500 MHz) radio frequency pulses were generated by a 2-kW Creative Electronics tube amplifier driven by a 50-W American Microwave Technology power amplifier. All final-stage amplifiers were under active control.[19] The π-pulse lengths were 9 μs for ^{13}C and ^1H. Proton-carbon-matched cross-polarization transfers were made in

(13) (a) deAzevedo, E. R.; Hu, W. G.; Bonagamba, T. J.; Schmidt-Rohr, K. *J. Am. Chem. Soc.* **1999**, *121*, 8411–8412. (b) deAzevedo, E. R.; Hu, W. G.; Bonagamba, T. J.; Schmidt-Rohr, K. *J. Chem. Phys.* **2000**, *112*, 8988–9001. (c) Reichert, D.; Bonagamba, T. J.; Schmidt-Rohr, K. *J. Magn. Reson.* **2001**, *151*, 129–135.
(14) Manolikas, T.; Herrmann, T.; Meier, B. H. *J. Am. Chem. Soc.* **2008**, *130*, 3959–3966.
(15) Weldeghiorghis, T. K.; Stueber, D.; Schaefer, J. *J. Polym. Sci., Part B: Polym. Phys.* **2008**, *46*, 1062–1066.
(16) Meier, B. H. *Polarization Transfer and Spin Diffusion in Solid-State NMR. In Advances in Magnetic and Optical Resonance*; Warren, W. S., Ed.; Academic Press: New York, 1994; Vol. 18, pp 1−116.
(17) VanderHart, D. L. *J. Magn. Reson.* **1987**, *72*, 13–47.
(18) Schaefer, J.; McKay, R. A. *U.S. Patent* **1999**, *5* (861), 748.
(19) Stueber, D.; Mehta, A. K.; Chen, Z.; Wooley, K. L.; Schaefer, J. *J. Polym. Sci. Phys.* **2006**, *44*, 2760–2775.

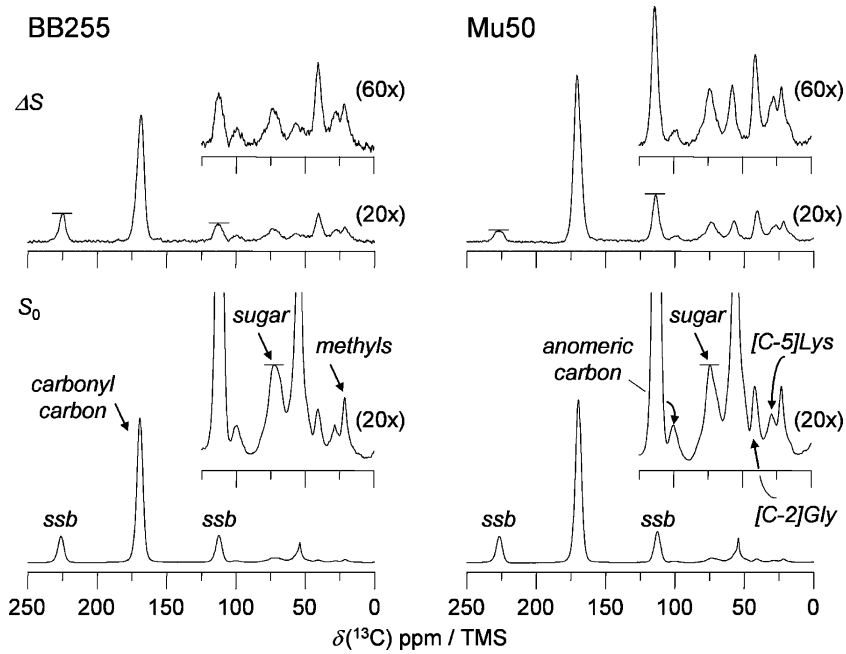

Figure 2. CODEX spectra of intact cell walls of *S. aureus* strains BB255 (left) and Mu50 (right) (both labeled by 99%-enriched [1-^{13}C]glycine) after a mixing time, $t_m = 840$ ms. The CODEX differences ($\Delta S = S_0 - S$) are at the top of the figure, and the CODEX references (S_0), at the bottom. The spectra have been normalized by the height of the sugar peak at 75 ppm. The spectra are the result of the accumulation of 131 072 scans. Magic-angle spinning was at 7143 Hz. Spinning sidebands are identified as "ssb."

2 ms at 56 kHz. Proton dipolar decoupling was 100 kHz during data acquisition.

Results

CODEX spectra for the cell walls of BB255 and Mu50 labeled by [1-^{13}C]glycine (99% isotopic enrichment) after a mixing time of 840 ms have similar S_0 spectra (Figure 2, bottom). This mixing time is sufficient to allow $^{13}C^1H^1H^{13}C$ spin diffusion over 5 Å.[17] The S_0 spectra are dominated by the 170-ppm peak from the ^{13}C-labeled carbonyl carbons of the pentaglycyl bridges. In the solid, the chemical shift assignments for the glycyl-carbonyl carbon in helix and in β-sheet are 171 and 168 ppm, respectively.[20,21] These differ from those in solution, where ~175 ppm is assigned for helix and ~172 ppm for β-sheet, with an average of 174.0 ppm for the glycyl-carbonyl carbon in proteins.[22] The glycycl-carbonyl carbon chemical shift is apparently highly sensitive to the change in the solid-state hydrogen-bonding pattern that results from changes in local conformation.[21a,b]

The resolved ^{13}C natural-abundance peaks include sugar carbons (100 and 75 ppm), the C-2 carbons of glycine and the C-6 carbon of lysine (42 ppm), the C-5 and C-3 carbons of lysine plus the C-3 and C-4 carbons of glutamine (30 ppm), and the methyl carbons of sugars and alanines (20 ppm).[23] All

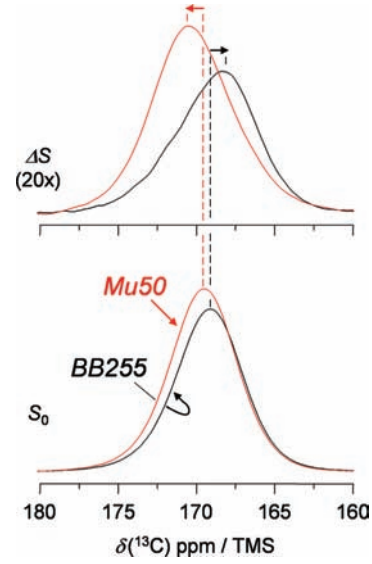

Figure 3. Expansion of the carbonyl-carbon regions of the spectra of Figure 2 showing that the CODEX differences for BB255 (black) and Mu50 (red) are shifted in frequency in opposite directions.

spectra have been normalized by the height of the sugar peak at 75 ppm, which can be considered an internal reference. The corresponding CODEX differences are somewhat more pronounced for the thicker cell wall of Mu50[12] (Figure 2, top) but the patterns are the same, with the exception that the carbonyl-carbon $n = \pm 1$ spinning sidebands are reversed in relative intensities in the two spectra (compare Figure 2, left and right), suggesting a difference in conformation. In addition, the frequencies of the carbonyl-carbon CODEX differences are shifted in opposite directions (Figure 3). When the mixing time is reduced to 280 ms, all the CODEX differences for both cell

(20) Saitô, H. *Magn. Reson. Chem.* **1986**, *24*, 835–852.
(21) (a) Ando, S.; Ando, I.; Shoji, A.; Ozaki, T. *J. Am. Chem. Soc.* **1988**, *110*, 3380–3386. (b) Nakano, J.; Kuroki, S.; Ando, I.; Kameda, T.; Kurosu, H.; Ozaki, T.; Shoji, A. *Biopolymers* **2000**, *54*, 81–88.
(22) Zhang, H.; Neal, S.; Wishart, D. S. *J. Biomol. NMR* **2003**, *25*, 173–195.
(23) (a) Meroueh, S. O.; Bencze, K. Z.; Hesek, D.; Lee, M.; Fisher, J. F.; Stemmler, T. L.; Mobashery, S. *Proc. Natl. Acad. Sci. U.S.A.* **2006**, *103*, 4404–4409. (b) Perez-Dorado, I.; Campillo, N. E.; Monterroso, B.; Hesek, D.; Lee, M.; Paez, J. A.; Garcia, P.; Martinez-Ripoll, M.; Garcia, J. L.; Mobashery, S.; Menendez, M.; Hermoso, J. A. *J. Biol. Chem.* **2007**, *282*, 24990–24999. (c) Cho, S.; Wang, Q.; Swaminathan, C. P.; Hesek, D.; Lee, M.; Boons, G.-J.; Mobashery, S.; Mariuzza, R. A. *Proc. Natl. Acad. Sci. U.S.A.* **2007**, *104*, 8761–8766.

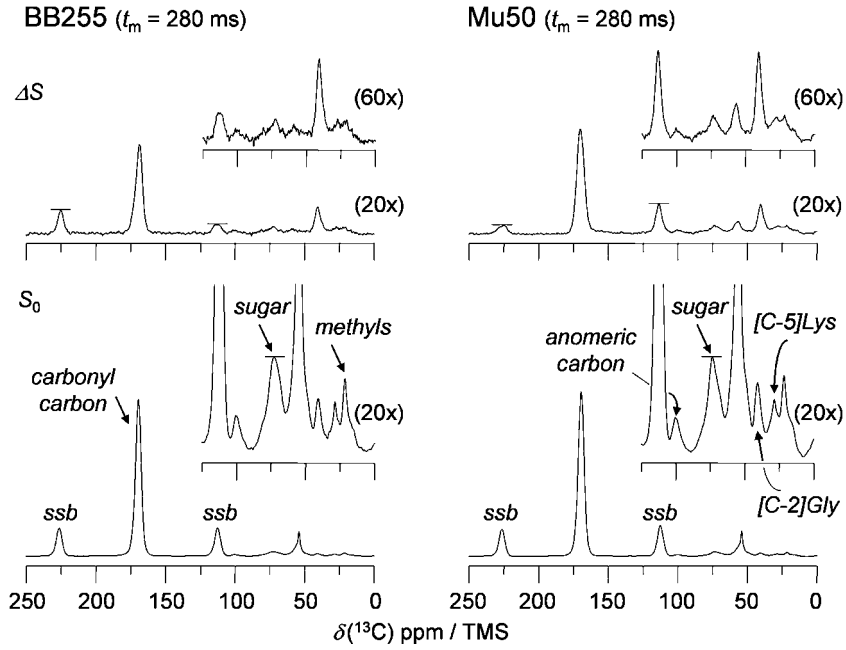

Figure 4. CODEX spectra of intact cell walls of *S. aureus* strains BB255 (left) and Mu50 (right) (both labeled by 99%-enriched [1-^{13}C]glycine) after a mixing time, $t_m = 280$ ms. The CODEX differences ($\Delta S = S_0 - S$) are at the top of the figure, and the CODEX references (S_0), at the bottom. Normalization is the same as in Figure 2. The spectra are the result of the accumulation of 131 072 scans. Magic-angle spinning was at 7143 Hz.

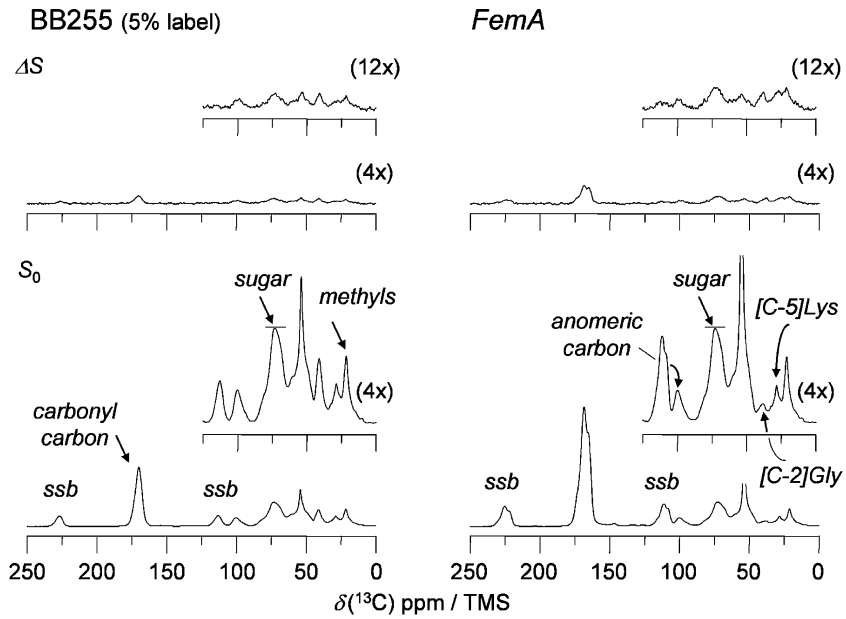

Figure 5. CODEX spectra of intact cell walls of *S. aureus* strain BB255 (labeled by 5%-enriched [1-^{13}C]glycine) shown on the left, and on the right, of mutant strain *FemA* (labeled by 99%-enriched [1-^{13}C]glycine), after a mixing time, $t_m = 840$ ms. The CODEX differences ($\Delta S = S_0 - S$) are at the top of the figure, and the CODEX references (S_0), at the bottom. Normalization is the same as in Figure 2. The spectra on the left are the result of the accumulation of 245 632 scans, and on the right, 166 272 scans. Magic-angle spinning was at 7143 Hz.

walls are reduced in intensity except those for the C-2 carbons of glycine at 42 ppm (Figure 4).

The carbonyl-carbon S_0 intensity for the cell walls of BB255 labeled by [1-^{13}C]glycine (5% isotopic enrichment) is reduced in intensity by more than a factor of 10, relative to that for cell walls labeled by fully enriched glycine (compare Figures 2 and 5, left panels). Nevertheless, the corresponding CODEX differences for the sugar carbons are only reduced by about a factor of 2, and those for the 42-, 30-, and 25-ppm peaks by factors of 3-4. In addition, the shift in frequency for the carbonyl-carbon CODEX difference relative to its S_0 spectra shown in Figure 3 has disappeared for the lower enrichment (Figure 6).

For *FemA* cell walls labeled by fully enriched glycine, the CODEX differences at 75 (but not 100), 30, and 25 ppm are greater than those for the cell walls of BB255 labeled by 5% enriched glycine (Figure 5, left and right). Both S_0 and ΔS at 42 ppm are reduced because *FemA* has only a single bridging glycyl residue (Scheme 1). The 42-ppm $\Delta S/S_0$ is ~35% (Figure 5, right), as expected for an isotopic enrichment of the bridge carbonyl carbon of 60-70%.

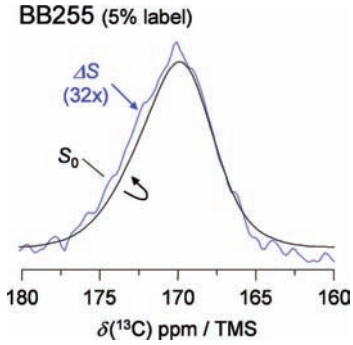

Figure 6. Expansion of the carbonyl-carbon region of the spectra of Figure 5 (left), showing that the CODEX difference is not shifted in frequency from that of its reference.

Discussion

Spin-Diffusion Rulers and Glycan Proximity to the Pentaglycyl Bridge. The observation of isotropic shift differences between ΔS and S_0 spectra for the pentaglycyl bridge glycyl carbonyl-carbon signals (Figure 3) alone is consistent with either slow motion or spin exchange for the 170-ppm peak. Disappearance of the shift difference upon isotopic dilution (Figure 6) rules out motion as the source of the CODEX difference.[15] The dilution also significantly decreases the intensities of the natural-abundance ^{13}C peaks between 20 and 100 ppm, confirming that they too are the result of ^{13}C spin diffusion and not molecular motion.

The 5% $\Delta S/S_0$ for the 170-ppm carbons of Figure 3 shows that one glycyl carbonyl-carbon $^{13}C-^{13}C$ pair undergoes a chemical-shift change during mixing for every two pentaglycyl bridges; that is $\Delta S/S_0 \approx (2/10)(1/2)(1/2) = 5\%$. The first factor of 1/2 is the probability the spin state of the $^{13}C-^{13}C$ pair has been changed by flip-flop exchange, and the second factor of 1/2 is the probability of finding adjacent carbonyl ^{13}C labels in the bridge for an isotopic enrichment of 60−70%.

Each natural-abundance glycyl C-2 carbon is directly bonded to one carbonyl carbon (1.5 Å separation), and is two bonds away from another (2.5 Å separation), distances assumed from X-ray structures of small molecular polypeptides.[24,25] With an isotopic glycyl carbonyl-carbon enrichment of ∼60%[7a] in the cell-wall isolates, the 42-ppm glycyl C-2 $\Delta S/S_0$ of about 60% indicates efficient exchange within $-^{13}CH_2-^{13}C(=O)-$ and $-^{13}C(=O)NH-^{13}CH_2-$ spin pairs.[17] (The incorporated enrichment is reduced from 99% by de novo glycine synthesis.) In addition, the 42-ppm $\Delta S/S_0$ is the same for both 280 and 840-ms mixing times (Figures 2 and 4), which means that the shorter mixing time is sufficient for spin exchange over two bonds. However, the 30-ppm $\Delta S/S_0$, which arises primarily from the C-5 carbon of L-lysine three bonds and 3−5 Å from a carbonyl-carbon label (Scheme 1), is less for the 280-ms mixing time than for the 840-ms mixing time (Figures 2 and 4).

This combination of results establishes an effective distance ruler for spin diffusion within the *S. aureus* cell-wall isolates. The observation of a CODEX difference for natural-abundance ^{13}C after a 280-ms mixing time, and an increase in that signal after an 840-ms mixing time, places that ^{13}C more than 2.5 Å and less than 5 Å from one of the ^{13}C labels of the pentaglycyl bridge. The sugar carbon-peaks at 75 and 100 ppm fall into this category (Figures 2 and 4). There are sugar carbons associated with wall teichoic acids, a polyglycerol phosphate polymer covalently attached to the cell-wall peptidoglycan through an *N*-acetylmannosamine-β(1−4)-*N*-acetylglucosamine linker,[26,27] but the low concentration of mannosamine in the cell wall isolates of *S. aureus*[28] means that teichoic-acid sugar concentrations are low and cannot account for the observed 75 and 100-ppm CODEX $\Delta S/S_0$ of more than 15%. We assign these CODEX differences to the glycan sugar carbons. Because the distance from the glycan mainchain to the pentaglycyl bridging segment of the same peptidoglycan repeat unit is more than 10 Å,[8c] the observed glycan-bridge distance necessarily is an inter-repeat-unit proximity (Figure 8, solid arrow) and so depends on the three-dimensional architecture of the peptidoglycan lattice.

Lattice Model for BB255. The glycan mainchain has a helical twist[5] so that peptide stems extend from the chain backbone in different directions. The proposal has been made before that the stems of *S. aureus* within a plane perpendicular to the glycan mainchain are antiparallel,[23a−c,29] and we now suggest that parallel stems are also a possibility. Parallel stems lead to a lattice in which adjacent stems are shifted in orientation by 90° and every fifth stem has the same orientation (Figure 7, left).

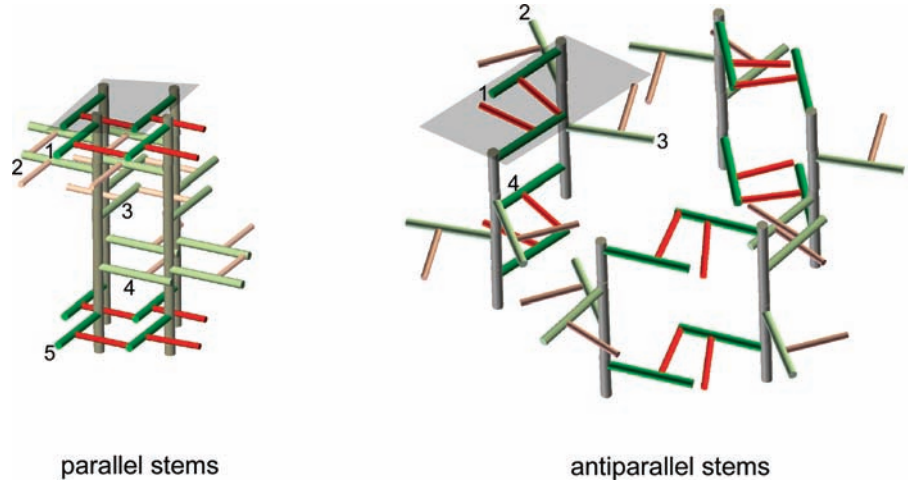

Figure 7. Peptidoglycan architecture for *S. aureus* in which coplanar stems (green) are either parallel (left), or antiparallel (right). Stems with the same orientation are highlighted in dark green for clarity. Bridges are in pink; highlighted bridges are red. The glycan backbones are brown. Every fifth stem has the same orientation on the left, and every fourth stem on the right. Coplanar parallel stems result in a densely packed lattice with the possibility of 100% cross-linking. Coplanar antiparallel stems are loosely packed with cross-linking that cannot exceed 50%. The gray planes are expanded in Figure 8.

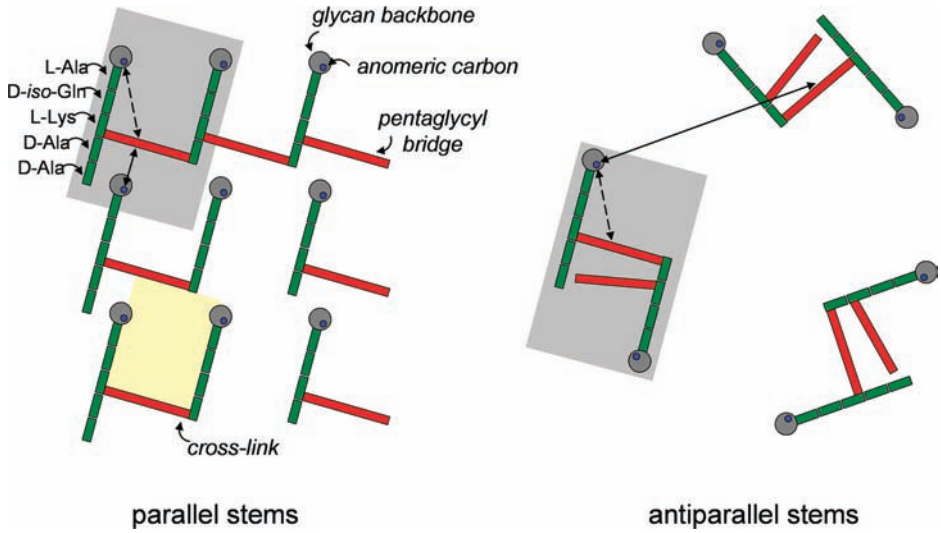

Figure 8. Cross sections of the petidoglycan structures of Figure 7. The cross-section on the left consists of 9 glycan chains in a 3 × 3 matrix, and that on the right, 6 glycan chains. The gray planes locate the cross sections relative to their 3-dimensional lattices in Figure 7. The glycan backbones (gray circles) are propagating into the plane of the paper. The stems and bridges are represented by green and red rectangles, respectively. Some of the bridges are missing on the left, reflecting the experimentally determined composition of the lattice (see refs 7a and 8a). The missing bridges increase the normal cross-sectional area between cross-linked stems, which is ~20 × 20 Å^2 (yellow square). The solid double-headed arrows indicate inter-repeat-unit distances between glycan sugars and bridging segments, and the dotted double-headed arrows, inta-repeat-unit distances.

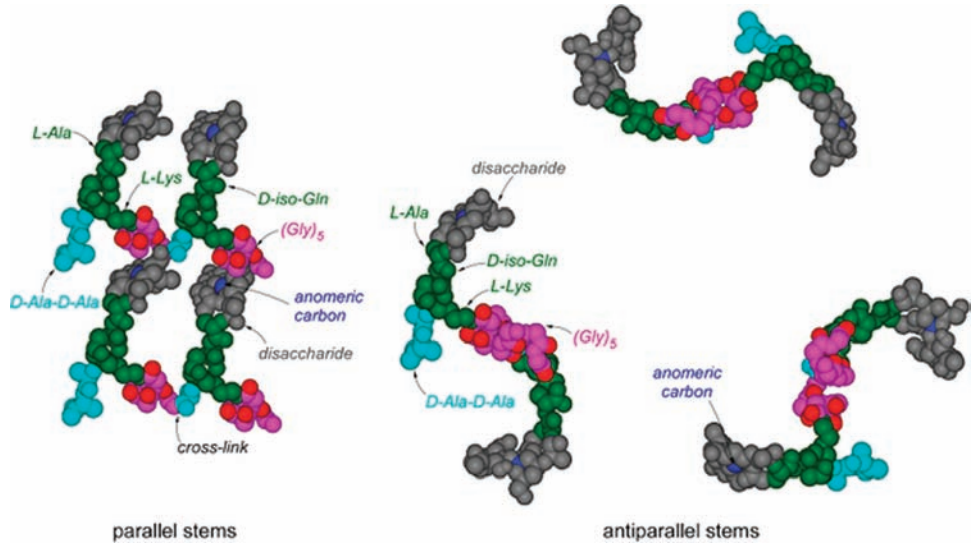

Figure 9. Space-filling models of the cross sections of Figure 8. Four parallel stems (green) are shown on the left, and six on the right. The D-alanine residues of the stems are in light blue, the pentaglycyl bridges in pink, the carbonyl carbons of the bridges in red, the glycan sugars in gray, and the anomeric carbons of the sugars in blue. The glycan mainchains are propagating into the plane of the paper. The anomeric sugar carbons are proximate to the glycyl carbonyl carbons in the cross-section on the left, but not in the cross-section on the right.

Antiparallel stems lead to a lattice in which adjacent stems are shifted in orientation by 120°, and every fourth stem has the same orientation (Figure 7, right). Cross sections of the two types of lattices show the parallel and antiparallel stems (Figure 8). The parallel stems are densely packed and can be 100% cross-linked, assuming an ideal chemical composition (no defects or missing components). Peptidoglycan fractions with cross-linking of 70% or more have been observed in *S. aureus*.[8c,30] In the 3-fold-symmetric peptidoglycan tertiary structure proposed for *E. coli* (which has no bridges) by Meroueh et al.,[23a−c] only one cross-link is formed between every two antiparallel stems, one acting as a cross-link donor and the other as a cross-link acceptor.[31] Hence, the maximum cross-linking is 50%. As shown in Figure 7 (right), an idealized 3-fold-symmetric model for *S. aureus* (which has bridges) is

(24) Hughes, E. W.; Moore, W. J. *Acta Crystallogr.* **1950**, *3*, 313.
(25) Zhang, S.; Prabpai, S.; Kongsaeree, P.; Arvidsson, P. I. *Chem. Commun.* **2006**, 497–499.
(26) Neuhaus, F. C.; Baddiley, J. *Microbiol. Mol. Biol. R.* **2003**, *67*, 686–723.
(27) Schertzer, J. W.; Brown, E. D. *J. Bacteriol.* **2008**, *190*, 6940–6947.
(28) Kojima, N.; Araki, Y.; Ito, E. *J. Biol. Chem.* **1983**, *258*, 9043–9045.
(29) Dmitriev, B. A.; Toukach, F. V.; Schaper, K. J.; Holst, O.; Rietschel, E. T.; Ehlers, S. *J. Bacteriol.* **2003**, *185*, 3458–3468.
(30) Snowden, M. A.; Perkins, H. R. *Eur. J. Biochem.* **1990**, *191*, 373–377.
(31) Driehuis, F.; De Jonge, B.; Nanninga, N. *J. Bacteriol.* **1992**, *174*, 2028–31.

less than 50% because one-third of the stems have no antiparallel neighboring stems in the same plane. The peptidoglycan lattice consists of loosely packed glycan chains (solid arrows, Figure 8, right) with 30-Å diameter holes.[23a−c,29]

Space-filling models of the two cross sections are shown in Figure 9. The tight packing of the parallel-stem model places the glycan sugar carbons (gray) of one repeat unit near the ^{13}C labels (red) of the pentaglycyl bridge of another unit. This proximity is impossible for the antiparallel stem model, either within a plane as illustrated or between planes which are separated by 10 Å or more. The CODEX-detected spin diffusion between bridge ^{13}C labels and natural-abundance glycan ^{13}C is inconsistent with the antiparallel stem model of Figure 7 for *S. aureus* and supports instead the parallel-stem model.

Lattice Models for *S. aureus* Mutants. Two conclusions emerge from the ^{13}C spin-diffusion measurements on the *S. aureus* mutant Mu50: (i) the average distance between nearest-neighbor bridge and glycan is reduced relative to that in BB255 and (ii) the conformation of the Mu50 bridge is kinked or coiled relative to that in BB255. The first conclusion is based on the direct comparison of intensities of the 75-ppm sugar-carbon CODEX ΔS peaks in Figure 2 (Mu50 peak intensity twice that of BB255) relative to those of the almost equal carbonyl-carbon S_0. The second conclusion is based on the ΔS downfield shift for Mu50 (Figure 3), and the correlations between downfield shifts for glycyl carbonyl carbons in peptides and coil conformations, and between upfield shifts and α-helix and β-strand conformations.[20,21a,b] We believe that the lattice structure for Mu50 is similar to that shown in Figure 7 (left), but with even closer packing made possible by kinked bridges. Such a structure is consistent with the known thicker cell wall of Mu50,[12] and its ability both to bind vancomycin (many uncross-linked stems), and still block access to the membrane exoface (reduced free volume).

The ^{13}C spin-diffusion measurements on the *S. aureus* mutant *FemA* show unequivocally that there is glycan-bridge proximity (Figure 5, right). However, the *FemA* bridging segment is so short (Scheme 1) that an all parallel-stem lattice model is impossible because of steric interference. An all antiparallel-stem lattice is also impossible because the observed glycan-bridge separation is less than 5 Å. That is, neither model of Figure 7 is directly applicable. Future model building for the *FemA* lattice must therefore reconcile the glycan-short bridge proximity by a rearrangement of the orientation of the stems.

Summary

The application of ^{13}C spin-diffusion measurements to intact cell-wall systems that have been specifically ^{13}C labeled provides atomic-level detail that is important for accurate model building of the architecture of the *S. aureus* peptidoglycan.

Acknowledgment. The authors thank Prof. Harald Labischinski (MerLion Pharmaceuticals GmbH, Robert-Rössle-Strasse 10, 13125 Berlin, Germany) and Prof. Brigitte Berger-Bächi (Universität Zürich, Institut für Medizinische Mikrobiologie, Switzerland) for providing wild-type *S. aureus* BB255 and its *fem*-deletion mutant, UK 17. This paper is based on work supported by the National Institutes of Health under Grant No. EB002058.

JA808971C